

K-Deep Simplex: Manifold Learning via Local Dictionaries

Abiy Tasissa¹, Pranay Tankala², James M. Murphy¹, and Demba Ba²

¹Department of Mathematics, Tufts University, Medford, MA

²School of Engineering and Applied Sciences, Harvard University, Cambridge, MA

January 18, 2023

Abstract

We propose *K-Deep Simplex (KDS)* which, given a set of data points, learns a dictionary comprising synthetic landmarks, along with representation coefficients supported on a simplex. KDS integrates manifold learning and sparse coding/dictionary learning: reconstruction term, as in classical dictionary learning, and a novel local weighted ℓ_1 penalty that encourages each data point to represent itself as a convex combination of nearby landmarks. We solve the proposed optimization program using alternating minimization and design an efficient, interpretable autoencoder using algorithm enrolling. We theoretically analyze the proposed program by relating the weighted ℓ_1 penalty in KDS to a weighted ℓ_0 program. Assuming that the data are generated from a Delaunay triangulation, we prove the equivalence of the weighted ℓ_1 and weighted ℓ_0 programs. If the representation coefficients are given, we prove that the resulting dictionary is unique. Further, we show that low-dimensional representations can be efficiently obtained from the covariance of the coefficient matrix. We apply KDS to the unsupervised clustering problem and prove theoretical performance guarantees. Experiments show that the algorithm is highly efficient and performs competitively on synthetic and real data sets.

1 Introduction

Consider observations of the form $(\mathbf{x}_i, \mathbf{y}_i)_{i=1}^n$ with $\mathbf{x}_i \in \mathcal{R}^m$ and $\mathbf{y}_i \in \mathcal{R}^d$ denoting predictor and response variables respectively. We assume that $\mathbf{y}_i = f(\mathbf{x}_i) + \varepsilon_i$ where ε_i represents random i.i.d noise. A ubiquitous model is the standard linear regression which first posits that f is linear and correspondingly estimates the model parameters via least squares. Rather than fixing a parametric model as in linear regression, non-parametric models learn the relation f from the data with minimal assumption on f (e.g. smoothness). One popular class of non-parametric models is the local linear regression model [43, 58, 14, 47]. In contrast to linear regression which assumes a global form of f , local regression is based on approximating f locally using linear functions. To be precise, the local linear fit at a point \mathbf{x}_i is defined using a weight function w_i that depends on distances to all other training data points i.e. less weight is assigned to points far from \mathbf{x}_i . Unlike the linear regression model where the global linear function is only needed for prediction at test point, the locally linear model depends on the adaptive weight function and hence is non-parametric. One downside of this model is the curse of dimensionality where locality defined via distance functions implies that the weight function either considers nearly no neighbors or nearly all neighbors. To circumvent this limitation, dimensionality reduction based approaches have been studied [24, 38]. Recent works have also explored local regression with new regularizations and recasting it as a optimization problem over a suitably defined graph [29, 72, 52].

In this paper, we consider the unsupervised learning problem where we only have access to high-dimensional data $(\mathbf{y}_i)_{i=1}^n$ with $\mathbf{y}_i \in \mathcal{R}^d$. This setting arises in many applications and the raw high-dimensional representation presents challenges for computation, visualization and analysis. The *manifold hypothesis* posits that many high-dimensional datasets can be approximated by a low-dimensional manifold or mixture thereof. Hereafter, a k -dimensional submanifold \mathcal{M} is a subset of \mathcal{R}^d which locally is a flat k -dimensional Euclidean space [37]. If the data lie on or near a *linear* subspace, principal component analysis (PCA) can be used to obtain a low-dimensional representation. But, PCA may fail to preserve nonlinear structures. Non-linear dimensionality reduction techniques [56, 61, 54, 8, 15] obtain low-dimensional representations while preserving local geometric structures of the data.

Our main motivation is to develop a model akin to local linear regression in the unsupervised setting. In fact, one of the critical parts of the local regression model is determining the neighborhood radius for each point such that the linear approximation is applied within the specified radius. We note that if the radius is set “large”, the linear approximation is sub-optimal. On the other hand, if the radius is set “small”, the locally linear estimate will be poor as it will only consider very few points. Given these extremes, determining the neighborhood radius, referred as the bandwidth function in the local regression literature [43], is of fundamental importance. A similar challenge also occurs in manifold learning algorithms in determining the number of neighbors (e.g. Locally Linear Embedding (LLE) [54]).

Herein, to build our model for the unsupervised setting, we use synthetic points for the locally linear approximation. To be precise, rather than considering the whole data and considering neighboring points, we build local approximations by employing synthetic points that are to be learned. This approach resembles archetypal analysis [17, 67] where data points $(\mathbf{y}_i)_{i=1}^n$ with $\mathbf{y}_i \in \mathcal{R}^d$ are expressed as a convex combination of points $\mathbf{a}_1, \mathbf{a}_2, \dots, \mathbf{a}_m$. The set of points $\{\mathbf{a}_i\}_{i=1}^m$ are known as the archetypes. In the original archetypal analysis paper [17], an alternating least squares problem is proposed to solve for the archetypes and the representation coefficients. To integrate archetypal analysis with local regression or manifold learning, we propose to represent each data point as a convex combination of archetypes with further regularization

enforcing that nearby archetypes are assigned more weight. One way to achieve this is by selecting a fixed number of archetypes. While simple, estimating the optimal number is challenging (as it inherently depends on the nonlinear structure of the data) and the resulting model is not flexible. Another way to impose locality is by enforcing that the weights are sparse for which the well-known ℓ_0 minimization is a natural regularizer. Given that ℓ_0 minimization is intractable, a widely adopted technique is based on its convex relaxation which yields the ℓ_1 regularizer. However, since the weights are supported on the simplex, all the feasible solutions attain the same ℓ_1 norm.

In this paper, we propose *K-Deep Simplex (KDS)*, a unified optimization framework for local archetypal learning. In KDS, each data point $\mathbf{y} \in \mathcal{R}^d$ is expressed as a sparse convex combination of m atoms. These atoms define a dictionary $\mathbf{A} \in \mathcal{R}^{d \times m}$ to be learned from the data. To glean intrinsically low-dimensional manifold structure, we regularize to encourage representing a data point using nearby atoms. The proposed method learns a dictionary \mathbf{A} and low-dimensional features with a structure imposed by convexity and locality of representation. To learn the atoms, we employ the alternating minimization framework which alternates between updating the atoms and updating the coefficients. The algorithm can also easily be mapped to a neural network architecture leading to interpretable neural networks. This mapping is along the lines of algorithm unrolling [64, 65, 62, 49], an increasingly popular technique for structured deep learning.

1.1 Contributions

This paper introduces a structured dictionary learning model based on the idea of representing data as a convex combination of local archetypes. One immediate advantage of the method is that it leads to an interpretable framework. Since the coefficients are non-negative and sum to 1, they automatically enjoy a probabilistic interpretation.

Another advantage of the proposed algorithm is its connection to structured compressive sensing. We show that the proposed locality regularizer can be interpreted as a weighted ℓ_1 relaxation for a suitably defined ℓ_0 minimization. Under a certain generative model of data, we show how the proposed weighted ℓ_1 norm exactly recovers the underlying true sparse solution. In contrast to standard compressive sensing which depends on coherence and restricted isometry property (which do not hold in our setting), the analysis hinges on intrinsic geometric properties of data.

The proposed locality regularizer is essentially a quadratic form of a Laplacian over a suitably defined graph. Since we learn a dictionary consisting of $m \ll n$ atoms, where m is independent of n and depends only on intrinsic geometric properties of the data, we show that the spectral embedding can be computed efficiently by only considering the $m \times m$ covariance matrix of the coefficient matrix.

We discuss various ways to solve the main optimization problem. In all the cases, we argue that in the typical setting where $m \ll n$, the proposed algorithm is scalable. In addition, since our KDS embedding can be computed efficiently, this naturally leads to a scalable spectral clustering algorithm. We provide theoretical performance guarantees for the clustering under a certain data model.

We also map our iterative algorithm to a structured neural network. This mapping is along the lines of iterative algorithm unrolling [12, 27, 53, 63, 64, 65, 62, 49] to solve our optimization problem. To be specific, we train a recurrent autoencoder with a nonlinearity that captures the constraint that our representation coefficients must lie on the probability simplex. To our knowledge, our use of algorithm unrolling for manifold learning is new.

For reproducibility, we will provide the code for all the experiments in this paper. To give a glimpse of the performance of KDS, Figure 1 shows the atoms the autoencoder learns for the classic two moons and MNIST datasets.

Differences from our prior works: Our previous work in [60] defines a weighted ℓ_0 norm and shows that the weighted ℓ_1 regularization studied in this paper recovers a unique solution under a certain generative model of data. Therein, we propose a simple alternating minimization algorithm to learn the sparse coefficients and the dictionary atoms and test it on two datasets. We remark on the differences between the work in [60] and current work:

1. We further consider the problem of recovery of dictionary atoms given fixed coefficients (Theorem 3).
2. A more general weighted ℓ_0 norm is defined (Definition 2).
3. We compare our method to more baselines and consider more datasets (Face dataset, hyperspectral data).
4. The main algorithm used in this paper is based on mapping the iterative algorithm to a neural network and departs from the previous algorithm.

We also note that parts of the current work has appeared in our previously unpublished paper [59]. In contrast to these prior works, the current work presents new theory, comparisons to more baselines, detailed review of related work and detailed interpretations of the proposed regularizer.

1.2 Notation

Lowercase and uppercase boldface letters denote column vectors and matrices, respectively. We denote the Euclidean, ℓ_0 , ℓ_1 norms of a vector \mathbf{x} , respectively as $\|\mathbf{x}\|_2$, $\|\mathbf{x}\|_0$ and $\|\mathbf{x}\|_1$. The Frobenius and operator norm of a matrix \mathbf{A} are respectively denoted as $\|\mathbf{A}\|_F$ and $\|\mathbf{A}\|$. The vector $\mathbf{1}$ denotes a vector whose entries are all 1. $\Delta^p \equiv \{\mathbf{z} \in \mathcal{R}^p : \sum_{i=1}^p z_i = 1, \mathbf{z} \geq \mathbf{0}\}$ denotes the probability simplex. Given a matrix \mathbf{A} , \mathbf{a}_i denotes the i -th column of \mathbf{A} . The set of $m \times n$ matrices where each column lies in the probability simplex Δ^m is denoted by \mathcal{S} . $\text{diag}(\mathbf{x})$ represents a diagonal matrix whose entries are the vector \mathbf{x} . Given a vector \mathbf{x} , $\mathbf{1}_{\mathbf{x}}$ denotes the vector whose i -th entry is 1 if $x_i > 0$ and is 0 otherwise. \mathbf{e}_j denotes a vector of zeros except a 1 in the j -th position. $\sigma_{\max}(\mathbf{A})$ denotes the largest singular value of \mathbf{A} .

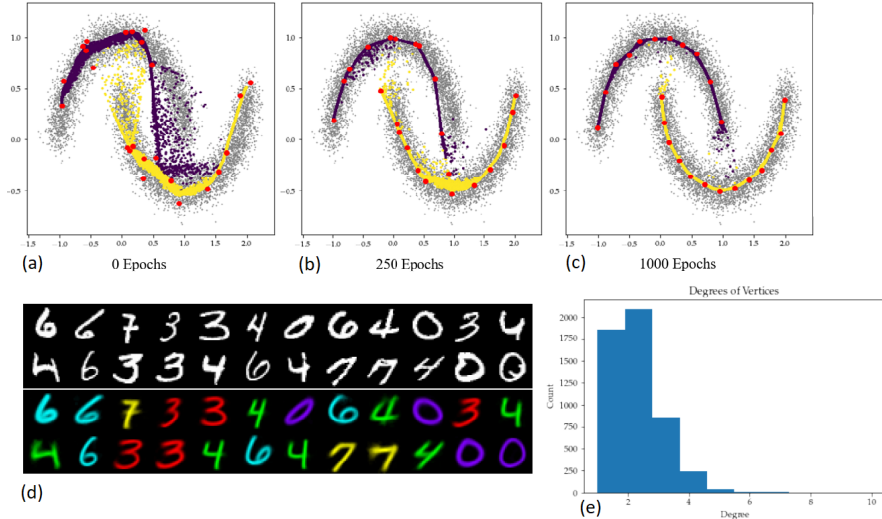


Figure 1: (a-c) Training from a random initialization of atoms on the two moons data set. (d) A subset of the randomly initialized atoms for MNIST (digits 0, 3, 4, 6, 7) before training (black and white) and after training and clustering (color). The number of data points is $n \approx 35000$ and the number of atoms is $m = 500$. (e) Degrees of vertices in the learned similarity graph. Despite being very sparse (most digits are represented using at most 5 atoms), the learned similarity graph retains enough information about the original data set that spectral clustering recovers these digits with 99% accuracy.

2 Proposed Method: K -Deep Simplex

Let $\mathbf{Y} = [\mathbf{y}_1, \dots, \mathbf{y}_n] \in \mathcal{R}^{d \times n}$ be a set of n data points in \mathcal{R}^d . Our approach is to approximate each data point \mathbf{y}_i by a convex combination of $m \ll n$ archetypes. We define a dictionary \mathbf{A} which is a collection of the m archetypes, $\mathbf{A} = [\mathbf{a}_1, \dots, \mathbf{a}_m] \in \mathcal{R}^{d \times m}$. For sake of presentation, we first consider the case where the data points can be represented exactly as a convex combination of the archetypes. This leads to $\mathbf{Y} = \mathbf{A}\mathbf{X}$ where $\mathbf{X} = [\mathbf{x}_1, \dots, \mathbf{x}_n] \in \mathcal{R}^{m \times n}$ is the coefficient or weight matrix. The convex combination implies $x_{ij} \geq 0$ for all i and j and $\mathbf{X}^\top \mathbf{1} = \mathbf{1}$. We note that this automatically provides us with a probabilistic interpretation of the coefficients. Next, we consider a suitable regularization with the aim that each data point is represented as a convex combination of its nearby archetypes. The regularization we consider is $\sum_{i,j} x_{ij} \|\mathbf{y}_i - \mathbf{a}_j\|^2$ where x_{ij} is the (j, i) -th entry of \mathbf{X} . The resulting optimization program is given by

$$\min_{\substack{\mathbf{A} \in \mathcal{R}^{d \times m} \\ \mathbf{X} \in \mathcal{S}}} \sum_{i,j} x_{ij} \|\mathbf{y}_i - \mathbf{a}_j\|^2 \quad \text{s.t. } \mathbf{Y} = \mathbf{A}\mathbf{X}, \quad (1)$$

2.1 KDS interpretations

Below, we further explore the objective in the optimization program in (1) by discussing various interpretations.

Graph matching: For a fixed \mathbf{A} , the objective in (1) can be related to graph matching. We consider matching the data points with the atoms using the coefficients to derive a cost matrix. Formally, we have the following

$$\min_{\mathbf{X} \in \mathcal{S}} \sum_{i,j} x_{ij} \|\mathbf{y}_i - \mathbf{a}_j\|^2 = \min_{\mathbf{X} \in \mathcal{S}} \text{trace}(\mathbf{X}^\top \mathbf{C}) = \min_{\mathbf{X} \in \mathcal{S}} \langle \mathbf{X}, \mathbf{C} \rangle,$$

where $\mathbf{C} \in \mathcal{R}_+^{m \times n}$ denotes a cost matrix defined as $C_{ij} = \|\mathbf{y}_i - \mathbf{a}_j\|_2^2$ and $\langle \mathbf{X}, \mathbf{C} \rangle$ denotes the trace inner product. The resulting problem is a one-sided linear assignment problem.

Optimal transport: Given the set of points \mathbf{Y} and \mathbf{A} , we define empirical measures $\mu_y = \frac{1}{n} \sum_{i=1}^n \delta_{\mathbf{y}_i}$ and $\mu_a = \frac{1}{m} \sum_{i=1}^m \delta_{\mathbf{a}_i}$ with δ denoting a Dirac measure. The squared Wasserstein-2 distance between the probability measures μ_y and μ_a is defined as

$$\mathcal{W}_2(\mu_y, \mu_a)^2 = \min_{\gamma \in \Pi(\mu_y, \mu_a)} \sum_{i=1}^n \sum_{j=1}^m \|\mathbf{y}_i - \mathbf{a}_j\|_2^2 \gamma_{ij},$$

where γ is the joint probability measure over $\mathbf{Y} \times \mathbf{A}$ and $\Pi(\mu_y, \mu_a) = \{\gamma \in \mathcal{R}^{n \times m} | \gamma \mathbf{1} = \mu_y, \gamma^\top \mathbf{1} = \mu_a\}$. If we let $\mathbf{X} = n\gamma^\top$, the squared Wasserstein distance is equivalent to minimizing the objective $\langle \mathbf{X}, \mathbf{C} \rangle$ over the set $\{\mathbf{X} \in \mathcal{R}_+^{n \times m} | \mathbf{X}^\top \mathbf{1}, \mathbf{X} \mathbf{1} = \frac{n}{m} \mathbf{1}\}$. In contrast to the standard regularizer which has one-sided constraint (sum to 1 constraint as a result of convex combination), this new formulation further restricts the sum of coefficients across rows placing a hard limit on how often a given atom is used to represent data points.

K-means: In the K-means problem, given dataset $\mathbf{Y} = [\mathbf{y}_1, \dots, \mathbf{y}_n] \in \mathcal{R}^{d \times n}$, we seek to simultaneously find m clusters with centers $\mathbf{A} = \{\mathbf{a}_1, \dots, \mathbf{a}_m\}$ and assign each data point to one of the m clusters. The optimization problem is

$$\min_{\mathbf{C}, \{\mathbf{a}_i\}_{i=1}^m} \sum_{j=1}^m \sum_{i=1}^n C_{ij} \|\mathbf{y}_i - \mathbf{a}_j\|_2^2,$$

where $C_{ij} \in \{0, 1\}$ is a binary assignment variable satisfying $\sum_{j=1}^m C_{ij} = 1$. The above minimization problem resembles the objective in (1). In fact, there is an optimal solution $(\mathbf{A}^*, \mathbf{X}^*)$ to $\min_{\mathbf{A} \in \mathcal{R}^{d \times m}, \mathbf{X} \in \mathcal{S}} \sum_{i,j} x_{ij} \|\mathbf{y}_i - \mathbf{a}_j\|^2$ where each column of \mathbf{X}^* is one-sparse i.e. \mathbf{X}^* is a binary assignment matrix.

Laplacian smoothness: We first define a set of vertices by combining the data points and atoms. The coordinate representation of the combined vertices is denoted by $\mathbf{R} = [\mathbf{Y} \ \mathbf{A}] \in \mathcal{R}^{d \times (n+m)}$. From this, we define a bipartite graph where edges only exist between data points and atoms i.e. in which an edge of weight x_{ij} connects the vertex \mathbf{y}_i and the vertex \mathbf{a}_j . The weight matrix $\mathbf{W} \in \mathcal{R}^{(n+m) \times (n+m)}$ is

$$\mathbf{W} = \begin{pmatrix} \mathbf{0} & \mathbf{X}^T \\ \mathbf{X} & \mathbf{0} \end{pmatrix}$$

The graph Laplacian is now defined as $\mathbf{L} = \mathbf{D} - \mathbf{W}$ where the diagonal degree matrix $\mathbf{D} \in \mathcal{R}^{(n+m) \times (n+m)}$ is defined as $D_{ii} = \sum_{j=1}^{n+m} W_{ij}$. We now show how the locality regularizer is connected to the quadratic form of the Laplacian.

$$\begin{aligned} & \sum_{i=1}^n \sum_{j=1}^m x_{ij} \|\mathbf{y}_i - \mathbf{a}_j\|_2^2 \\ &= \sum_{i=1}^n \mathbf{y}_i^T \mathbf{y}_i \sum_{j=1}^m x_{ij} + \sum_{j=1}^m \mathbf{a}_j^T \mathbf{a}_j \sum_{i=1}^n x_{ij} - 2 \sum_{i=1}^n \sum_{j=1}^m x_{ij} \mathbf{y}_i^T \mathbf{a}_j \\ &= \text{trace}(\mathbf{Y}^T \mathbf{Y} \mathbf{I}) + \text{trace}(\mathbf{A}^T \mathbf{A} \text{diag}(\mathbf{X} \mathbf{1})) - 2 \text{trace}(\mathbf{R}^T \mathbf{R} \mathbf{W}) \\ &= \text{trace}(\mathbf{R}^T \mathbf{R} \mathbf{D}) - \text{trace}(\mathbf{R}^T \mathbf{R} \mathbf{W}) \\ &= \text{trace}(\mathbf{R}^T \mathbf{R} (\mathbf{D} - \mathbf{W})) = \text{trace}(\mathbf{R} \mathbf{L} \mathbf{R}^T) \end{aligned}$$

Hence, the summation is precisely the *Laplacian quadratic form* of the graph, evaluated on the function mapping vertices of the graph to their corresponding positions in \mathcal{R}^d .

3 Related Works

3.1 Locality constrained dictionary learning

Our work connects with sparse coding and dictionary learning. In sparse coding, given a fixed *dictionary* $\mathbf{A} \in \mathcal{R}^{d \times m}$ of m atoms, a data point $\mathbf{y} \in \mathcal{R}^d$ is represented as a linear combination of at most $k \ll m$ columns of \mathbf{A} . The dictionary \mathbf{A} can be predefined [9] (e.g. Fourier bases, wavelets, curvelets) or adaptively learned from the data [22, 5, 6, 45]. The latter setting where the dictionary is simultaneously estimated with the sparse coefficients is the standard dictionary learning problem. We consider the prototypical form of the optimization objective for dictionary learning $\sum_{i=1}^n \frac{1}{2} \|\mathbf{y}_i - \mathbf{A} \mathbf{x}_i\|_2^2 + R(\mathbf{x}_i, \mathbf{A})$ where $R(\mathbf{x}_i, \mathbf{A})$ is a regularization term on the representation coefficients and the dictionary atoms.

In Table 1, we review related works in graph regularized coding and locality constrained coding. The main idea in these works is to employ a Laplacian smoothness regularization such that if two data points are close, the regularization encourages their coefficients to be similar [20, 11]. A few remarks are in order in how KDS compares to these methods. First, in KDS regularization, the underlying graph is not fixed but iteratively updated since the weights of the graph depend on the sparse representation coefficients. This is in contrast to methods that consider $\text{trace}(\mathbf{X} \mathcal{L} \mathbf{X}^T)$ where \mathcal{L} is a priori fixed based on similarity of the data points. In Table 1, the closest methods to KDS are [30, 76, 69, 21]. However, the coefficients in these methods do not lie on the simplex and the regularizers are based on x_{ij}^2 or $|x_{ij}|$. The implication of this is that the sparse coding step for [30, 69] yields a unique solution which departs from the KDS setup where uniqueness is not guaranteed under general conditions. The sparse manifold clustering and embedding algorithm (SMCE) [21] employs proximity regularization that promotes using neighborhood points. A drawback of SMCE is its computational inefficiency since it uses a dictionary constituted from the data points. We also note that the theoretical analysis presented in this paper is intimately connected to the simplex structure on the coefficients. It is not immediately clear how this analysis can be adapted to the case when the coefficients can have negative entries. Finally, the work in [78] proposes a similar regularization to ours with the authors referring to it as “adaptive distance regularization”. However, the methodology therein is based on using the data matrix as a dictionary and lacks theoretical analysis. Finally, we refer the reader to [1] to find a comprehensive overview of nonlinear manifold clustering algorithms.

3.2 Manifold learning

Our setup is along the lines of methods that learn local or global features of data using neighborhood analysis. For instance, Locally Linear Embedding (LLE) [54] provides a low dimensional embedding using weights that are defined as the reconstruction coefficients of data points from their neighbors. The choice of the optimal neighborhood size is important for LLE as it determines the features obtained and subsequently the performance of downstream tasks. Geometric multiresolution analysis (GMRA) is a fast and efficient algorithm that learns multiscale representations of the data based on local tangent space estimations [6, 45]. Since the dictionary elements used to reconstruct are defined locally, GMRA is not immediately useful for global downstream tasks, e.g. clustering. We also note that the work in [39] develops a theoretical framework for regression on low-dimensional sets embedded in high dimensions. The regression is done via local polynomial fitting which resembles local convex approximation in KDS albeit the former method applying in the supervised setting.

Table 1: related work

Work	$R(\mathbf{X})$	Notes
[77]	$\text{trace}(\mathbf{X}\mathcal{L}\mathbf{X}^T) + \lambda\ \mathbf{X}\ _1$	Sparse \mathbf{X} and $\ \mathbf{a}_i\ _2^2 \leq c$ \mathcal{L} priori fixed
[31]	None	Simplex constraints on X
[30]	$\text{trace}(\mathbf{X}\mathcal{L}\mathbf{X}^T)$	\mathcal{L} priori fixed
[69]	$\sum_{i,j} x_{ij}^2 \exp\left(\frac{2\ \mathbf{y}_i - \mathbf{a}_j\ }{\sigma}\right)$	$\mathbf{X}^T \mathbf{1} = \mathbf{1}$ and $\ \mathbf{a}_i\ _2^2 \leq c$
[79]	$\sum_{i,j} x_{ij}^2 \ \mathbf{y}_i - \mathbf{a}_j\ ^2 + \lambda\ \mathbf{X}\ _F^2$	$\mathbf{X}^T \mathbf{1} = \mathbf{1}$, x_{ij} set to zero based on neighborhood
[33]	$\text{trace}(\mathbf{X}\mathcal{L}\mathbf{X}^T) + \lambda\ \mathbf{X}\ _0$	Sparse \mathbf{X} , \mathcal{L} priori fixed
[76]	$\sum_{i,j} x_{ij} \ \mathbf{y}_i - \mathbf{a}_j\ ^{1+p}$	$\mathbf{X}^T \mathbf{1} = \mathbf{1}$.
[74]	$\text{trace}(\mathbf{X}^T \mathcal{L} \mathbf{X})$	$\ \mathbf{a}_i\ ^2 = 1$. An additional SVM regularization
[78]	$\sum_{i,j} x_{ij} \ \mathbf{y}_i - \mathbf{y}_j\ ^2 + \ \mathbf{X}\ _F^2$ $\text{diag}(\mathbf{X}) = \mathbf{0}$	Simplex constraints, No dictionary learning
[21]	$\sum_{i,j} Q_{ij} x_{ij}$	$\mathbf{X}^T \mathbf{1} = \mathbf{1}$ $\mathbf{Q} \equiv$ proximity regularizer

3.3 Scalable manifold learning via landmarks

For large datasets, the embedding step in manifold learning techniques which typically involves a spectral problem can be costly. One approach to circumvent the computational challenge is based on finding an approximate solution by first identifying a subset of points designated as landmarks or exemplars. For instance, the works in [57, 18] propose landmark isometric feature mapping (Isomap) and landmark multidimensional scaling (MDS) which are scalable versions of Isomap [61] and classical MDS. An approach along the lines of our work is the work in [68] which proposes an efficient version of the locally linear embedding method using landmarks. In contrast to our approach which learns the landmarks, we note that this method identifies the landmarks from the full data using strategies such as random sampling and clustering. A method inspired by LLE for semi-supervised learning, Local Anchor Embedding (LAE), is proposed in [41]. In this approach, the anchors are centers learned from the K-means algorithm. To obtain the representation coefficient of each data point, LAE solves a least squares problem in a dictionary of s -nearest anchors and with coefficients restricted on the simplex. Compared to our approach, the anchor learning step is disjoint from the sparse coding step in LAE. In addition, while LAE introduces sparsity by setting number of nearest anchors, our approach is based on promoting sparsity via a flexible proximity regularization. There are scalable landmark/exemplar methods for sparse subspace clustering e.g. [75, 3, 46] but subspace clustering stipulates global affine structure that is not directly applicable to the general case of nonlinear manifolds.

3.4 Non-negative matrix factorization

Non-negative matrix factorization (NMF) considers the problem of approximating a nonnegative data matrix using underlying components that are also non-negative [35, 25]. Formally, given a data matrix $\mathbf{Y} \in \mathcal{R}_+^{d \times n}$, approximate NMF seeks non-negative matrices $\mathbf{W} \in \mathcal{R}_+^{d \times m}$ and $\mathbf{H} \in \mathcal{R}_+^{m \times n}$ that best approximate the data. Choosing the Euclidean distance as a loss function, the problem can be formulated as $\min_{\mathbf{W} \in \mathcal{R}_+^{d \times m}, \mathbf{H} \in \mathcal{R}_+^{m \times n}} \|\mathbf{Y} -$

$\mathbf{WH}\|_F^2$. Different models on NMF put forth various conditions on the data matrix and the components. The work in [19] proposes a convex-model for NMF for a general data matrix with the restriction that \mathbf{H} is non-negative and the columns of \mathbf{W} lie in the column space of \mathbf{Y} . A closest work to our appears in [40] where the authors propose simplex structured matrix factorization (SSMF) which considers the recovery of \mathbf{W} and \mathbf{H} given a generic data matrix with the restriction that $\mathbf{H} \in S$. Therein, the authors show that the exact \mathbf{W} can be recovered by considering the a maximum volume ellipsoid inscribed in the convex hull of the data points. We note that the model assumption in [40] assumes a full column rank \mathbf{A} and a full row rank \mathbf{X} which we do not assume in our setting. Further discussion of different assumptions for identifiability of SSMF can be found in [2]. Finally, the works in [26] and [13] in hyperspectral imagery study a similar problem as ours but with the difference that the former considers a non-negative constraint and the latter uses the ℓ_0 regularizer on the simplex.

4 Theoretical analysis

To solve the optimization program in (1), a common approach is alternating minimization which is comprised of two steps. The first is sparse coding and the second step is dictionary learning. In this section, we provide theoretical analysis for the sparse coding and dictionary learning steps of our proposed optimization program in (1). These are respectively the sub-problems obtained by fixing \mathbf{A} and \mathbf{X} and optimizing for \mathbf{X} and \mathbf{A} respectively. We also discuss how to obtain low dimensional embedding of data points. Part of this analysis was completed in our prior work in [60].

4.1 Sparse coding

The theoretical analysis for the sparse coding step assumes a certain data model. To be precise, we consider m landmark points $\mathbf{a}_1, \mathbf{a}_2, \dots, \mathbf{a}_m$ with a unique Delaunay triangulation [36] and assume that each data point

in the set $\{\mathbf{y}_i\}_{i=1}^n \in \mathcal{R}^d$ is generated from a convex combination of at most $d + 1$ atoms. We give a precise definition of Delaunay triangulation below

Definition 1. A triangulation of n points $\mathbf{P} = \{\mathbf{p}_1, \mathbf{p}_2, \dots, \mathbf{p}_m\}$ in \mathcal{R}^d is called a Delaunay triangulation, if the circumsphere of every triangle does not contain no other point of \mathbf{P} .

The important property of this triangulation is that no point among the landmarks is inside the circumsphere of any triangle. This leads to well-separated landmarks, a property which is crucial for the analysis. Figure 2 shows an example with $d = 2$ i.e. data points in \mathcal{R}^2 . Compactly, we have $\mathbf{y}_i = \mathbf{A}\mathbf{x}_i$ where the $d \times m$ matrix \mathbf{A} is the dictionary defined as $\mathbf{A} = [\mathbf{a}_1, \mathbf{a}_2, \dots, \mathbf{a}_m]$ and $\mathbf{x}_i \in \Delta^m$. Our aforementioned goal of

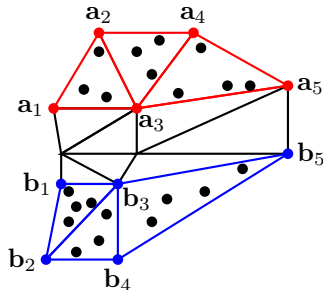


Figure 2: The red dots indicate the atoms which generate the data points. Each black dot, denoting a data point, is a convex combination of three atoms which are vertices of the triangle the point belongs to. We show that the optimal weighted ℓ_0 and ℓ_1 norm is based on a point representing itself using the vertices of the triangle it belongs to.

representing by local dictionaries motivates the following definition of a weighted ℓ_0 pseudo-norm.

Definition 2. Assume m landmark points $\mathbf{a}_1, \mathbf{a}_2, \dots, \mathbf{a}_m$ in \mathcal{R}^d have a unique Delaunay triangulation. Let the point $\mathbf{z} \in \mathcal{R}^d$ have the following representation, $\mathbf{z} = \sum_{i=1}^m x_i \mathbf{a}_i$ with the coefficient vector \mathbf{x} supported on the probability simplex in \mathcal{R}^m . Let \mathbf{z} belong to a Delaunay cell with center \mathbf{c} . The weighted ℓ_0 norm is defined as

$$\ell_{W,0}(\mathbf{x}) = \sum_{i=1}^m \frac{\mathbf{1}_{\mathbf{x}}}{\|\mathbf{x}\|_0} \|\mathbf{c} - \mathbf{a}_i\|^2, \quad (2)$$

Given the above definition of a weighted ℓ_0 norm and the fact that a given point \mathbf{z} admits different representations as a convex combination of the dictionary atoms, the natural question is the sense in which this norm is minimal i.e. among the different representations, which ones admit minimal values in this norm? The following theorem shows that the local reconstruction is minimal in the weighted ℓ_0 norm.

Theorem 1. Let $\mathbf{y} \in \mathcal{R}^d$ lie in the convex hull of the points $\mathbf{a}_1, \dots, \mathbf{a}_m \in \mathcal{R}^d$ with a unique Delaunay triangulation. Let \mathbf{y} belong to a Delaunay cell with center \mathbf{c} and radius R . Consider the following $\ell_{W,0}$ minimization problem.

$$\min_{\mathbf{x} \in \Delta^m} \ell_{W,0}(\mathbf{x}) \quad \text{s.t.} \quad \mathbf{y} = \mathbf{A}\mathbf{x}.$$

The optimal solution \mathbf{x}^* to the above program is such that $\mathbf{x}_j^* \neq 0$ comprise the vertices of some face of this triangulation that contains \mathbf{y} .

Proof. Consider an arbitrary Delaunay cell containing \mathbf{y} defined by the vertices $\{\mathbf{a}_j : j \in T, |T| = k\}$ with $T \subseteq [m]$ denoting a set of at most $d + 1$ indices. Using vertices in T , \mathbf{y} can be represented as a convex combination using coefficient vector \mathbf{x}^* . Let \mathbf{x} be another feasible solution of the program with support T' . By the definition of a Delaunay cell, there is a sphere with center \mathbf{c} and radius r such that $\|\mathbf{a}_j - \mathbf{c}\| = R$ for each $j \in T$ and $\|\mathbf{a}_j - \mathbf{c}\| > R$ for each $j \notin T$. It follows that

$$\begin{aligned} \sum_{i \in T'} \frac{\mathbf{1}_{\mathbf{x}}}{\|\mathbf{x}\|_0} \|\mathbf{c} - \mathbf{a}_i\|^2 &> R^2 \sum_{i \in T'} \frac{\mathbf{1}_{\mathbf{x}}}{\|\mathbf{x}\|_0} = R^2 \sum_{i \in T} \frac{\mathbf{1}_{\mathbf{x}^*}}{\|\mathbf{x}^*\|_0} \\ &= \sum_{i \in T} \frac{\mathbf{1}_{\mathbf{x}^* \neq 0}}{\|\mathbf{x}^*\|_0} \|\mathbf{c} - \mathbf{a}_i\|^2 \end{aligned}$$

Above, the inequality follows from the fact that atoms within T are the closest to the point \mathbf{c} . Therefore, the k -sparse representation using the vertices in T is the optimal solution to the $\ell_{W,0}$ minimization problem. \square

Given a reconstruction $\mathbf{y} = \mathbf{A}\mathbf{x}$, we note that the weighted ℓ_0 norm puts a uniform prior on all atoms which are used in the representation. Motivated by the fact that the weighted ℓ_0 norm enforces local reconstructions and with the goal of obtaining a regularization amenable to optimization, one could define a convex relaxation $\sum_{i=1}^m x_i \|\mathbf{c} - \mathbf{a}_i\|^2$ where the uniform prior has been replaced with entries of \mathbf{x} . However, when using \mathbf{x} as weights, the regularizer could strongly be formulated in terms of the point \mathbf{y} rather than the center of the triangulation it belongs to. This has to do with the fact that the weights in convex combination sum to 1 and are also proportional to the distance to the atoms. With that, we now define a convex relaxation of the weighted ℓ_0 problem as follows.

Definition 3. Assume m landmark points $\mathbf{a}_1, \mathbf{a}_2, \dots, \mathbf{a}_m$ in \mathcal{R}^d have a unique Delaunay triangulation. Let the point $\mathbf{z} \in \mathcal{R}^d$ have the following representation, $\mathbf{z} = \sum_{i=1}^m x_i \mathbf{a}_i$ with the coefficient vector \mathbf{x} supported on the probability simplex in \mathcal{R}^m . The weighted ℓ_1 norm is defined as

$$\ell_{W,1}(\mathbf{x}) = \sum_{i=1}^m x_i \|\mathbf{z} - \mathbf{a}_i\|^2, \quad (3)$$

Analogous to compressive sensing theory, the next question is the sense in which a weighted ℓ_1 minimization is equivalent to a weighted ℓ_0 minimization problem. This equivalency is summarized in the theorem below.

Theorem 2. Let $\mathbf{y} \in \mathcal{R}^d$ lie in the convex hull of the points $\mathbf{a}_1, \dots, \mathbf{a}_m \in \mathcal{R}^d$ with a unique Delaunay triangulation. Consider the following $\ell_{W,1}$ minimization problem.

$$\min_{\mathbf{x} \in \Delta^m} \sum_j x_j \|\mathbf{y} - \mathbf{a}_j\|^2 \quad \text{s.t.} \quad \mathbf{y} = \mathbf{A}\mathbf{x}.$$

The optimal solution \mathbf{x}^* to the above program is such that $\mathbf{x}_j^* \neq 0$ comprise the vertices of some face of this triangulation that contains \mathbf{y} .

Proof. Consider an arbitrary Delaunay cell containing \mathbf{y} defined by the vertices $\{\mathbf{a}_j : j \in T, |T| = k\}$ with $T \subseteq [m]$ denoting a set of at most $d + 1$ indices. Using vertices in T , \mathbf{y} can be represented as a convex combination using coefficient vector \mathbf{x}^* . Let \mathbf{x} be another feasible solution of the program with support T' . By the definition of a Delaunay cell, there is a sphere with center \mathbf{c} and radius R such that $\|\mathbf{a}_j - \mathbf{c}\| = R$ for each $j \in T$ and $\|\mathbf{a}_j - \mathbf{c}\| > R$ for each $j \notin T$.

Observe that for any vector $\mathbf{c} \in \mathcal{R}^d$, the identities $\mathbf{y} = \sum_j x_j \mathbf{a}_j$ and $\sum_j x_j = 1$ imply

$$\begin{aligned} & \sum_j x_j \|\mathbf{y} - \mathbf{a}_j\|^2 \\ &= \sum_j x_j (\|\mathbf{a}_j - \mathbf{c}\|^2 - 2\langle \mathbf{y} - \mathbf{c}, \mathbf{a}_j - \mathbf{c} \rangle + \|\mathbf{y} - \mathbf{c}\|^2) \\ &= \sum_j x_j \|\mathbf{a}_j - \mathbf{c}\|^2 - \|\mathbf{y} - \mathbf{c}\|^2. \end{aligned}$$

The above identity also holds if we replace x_j with x_j^* . We now consider the value of the objective using the coefficient vector \mathbf{x}

$$\begin{aligned} \sum_{j \in T'} x_j \|\mathbf{y} - \mathbf{a}_j\|^2 &= \sum_{j \in T'} x_j \|\mathbf{a}_j - \mathbf{c}\|^2 - \|\mathbf{y} - \mathbf{c}\|^2 \\ &< \sum_{j \in T'} x_j R^2 - \|\mathbf{y} - \mathbf{c}\|^2 \\ &= \sum_{j \in T} x_j^* \|\mathbf{a}_j - \mathbf{c}\|^2 - \|\mathbf{y} - \mathbf{c}\|^2 \\ &= \sum_{j \in T} x_j^* \|\mathbf{y} - \mathbf{a}_j\|^2, \end{aligned}$$

which confirms the optimality of \mathbf{x}^* . Thus, each point \mathbf{a}_j such that $x_j^* \neq 0$ is a vertex of the cell. Hence, $\{\mathbf{a}_j : x_j^* \neq 0\}$ are the vertices of some face of the triangulation containing \mathbf{y} . \square

4.2 Optimal dictionary

Assume that the sparse coefficients are fixed, we consider the following minimization problem to learn \mathbf{A}

$$\min_{\mathbf{A} \in \mathcal{R}^{d \times m}} \|\mathbf{Y} - \mathbf{A}\mathbf{X}\|_F^2 + \lambda \sum_{i=1}^n \sum_{j=1}^m x_j \|\mathbf{y}_i - \mathbf{a}_j\|^2, \quad (4)$$

where λ is a regularization parameter. Below, we will prove that there is a unique dictionary \mathbf{A} that solves (4).

Theorem 3. For fixed $\mathbf{X} \in S$, the minimization problem in (4) over the dictionaries \mathbf{A} yields a unique solution.

Proof. For fixed $\mathbf{X} \in S$, we consider the gradient of the objective function in (4). Let $f(\mathbf{A})$ denote the objective function. Some calculation yields $\nabla f(\mathbf{A}) = (\mathbf{A}\mathbf{X} - \mathbf{Y})\mathbf{X}^T + 2\lambda\mathbf{A}\text{diag}(\mathbf{X}\mathbf{1}) - 2\lambda\mathbf{Y}\mathbf{X}^T$. We first argue that the objective is strongly convex by showing that $\langle \nabla f(\mathbf{A}_1) - \nabla f(\mathbf{A}_2), \mathbf{A}_1 - \mathbf{A}_2 \rangle \geq \mu \|\mathbf{A}_1 - \mathbf{A}_2\|_F^2$ with $\mu > 0$ for any $\mathbf{A}_1, \mathbf{A}_2$. Using the explicit form of the gradient, strong convexity is equivalent to showing that $\langle \mathbf{X}\mathbf{X}^T + 2\lambda\text{diag}(\mathbf{X}\mathbf{1}), (\mathbf{A}_1 - \mathbf{A}_2)^T (\mathbf{A}_1 - \mathbf{A}_2) \rangle \geq \mu \|\mathbf{A}_1 - \mathbf{A}_2\|_F^2$. For ease of notation, let $\mathbf{H} = \mathbf{X}\mathbf{X}^T + 2\lambda\text{diag}(\mathbf{X}\mathbf{1})$ and $\mathbf{G} = (\mathbf{A}_1 - \mathbf{A}_2)^T (\mathbf{A}_1 - \mathbf{A}_2)$. We first note that \mathbf{H} is symmetric positive definite and \mathbf{G} is symmetric positive semidefinite. To see the former claim, it suffices to show that the diagonal entries of $\text{diag}(\mathbf{X}\mathbf{1})$ are non-zero. The only case an entry will be zero is if an atom is not used by all data points. For this case, the given atom can be discarded. In all other cases, all the diagonal entries of $\text{diag}(\mathbf{X}\mathbf{1})$ are positive. Finally, we claim that $\langle \mathbf{H}, \mathbf{G} \rangle \geq \lambda_{\min}(\mathbf{H}) \text{trace}(\mathbf{G})$. This gives the desired strong convexity result with $\mu = \lambda_{\min}(\mathbf{H}) > 0$. Setting the gradient to zero yields the unique solution $\mathbf{A}^* = (1 + 2\lambda)\mathbf{H}^{-1}(\mathbf{Y}\mathbf{X}^T)$.

It remains to prove the claim that $\langle \mathbf{H}, \mathbf{G} \rangle \geq \lambda_{\min}(\mathbf{H}) \text{trace}(\mathbf{G})$. This follows from noting that the matrix $\mathbf{H} - \lambda_{\min}(\mathbf{H})\mathbf{I}$ is symmetric positive semidefinite and the term $\langle \mathbf{H} - \lambda_{\min}(\mathbf{H})\mathbf{I}, \mathbf{G} \rangle \geq 0$ as it is a trace product of symmetric positive semidefinite matrices.

Remarks: We note that the weighted ℓ_1 regularizer enables us to obtain strong convexity when optimizing over the dictionary atoms. If $\lambda = 0$, strong convexity is not always guaranteed. If we ignore the reconstruction term ($\lambda \rightarrow \infty$) and set each of the sparse coefficient to be 1-sparse, some calculation yields that we obtain the optimal atoms to be the K -means centroids. \square

4.3 KDS Embedding

The representation coefficients $\mathbf{X} \in S$ computed by KDS implicitly define a bipartite *similarity graph* G with $n + m$ vertices corresponding to the n data points and m learned dictionary atoms. In this graph, each data point \mathbf{y}_i and each atom \mathbf{a}_j is connected by an undirected edge of weight x_{ij} . To embed the data points and the atoms into \mathcal{R}^k , we consider the classic spectral embedding.

$$\min_{\mathbf{Q} \in \mathcal{R}^{k \times (n+m)}} \text{trace}(\mathbf{Q}\mathbf{L}\mathbf{Q}^T) \quad \text{s.t. } \mathbf{Q}\mathbf{1} = \mathbf{0}, \quad \mathbf{Q}\mathbf{Q}^T = \mathbf{I} \quad (5)$$

where $\mathbf{Q} = [\mathbf{Q}_Y \quad \mathbf{Q}_A] \in \mathcal{R}^{k \times (n+m)}$. We enforce an additional constraint $\mathbf{Q}_Y = \mathbf{Q}_A \mathbf{X}$. This is quite natural since our sparse coefficient matrix \mathbf{X} approximately satisfies $\mathbf{Y} = \mathbf{A}\mathbf{X}$. We now expand $\text{trace}(\mathbf{Q}\mathbf{L}\mathbf{Q}^T)$.

$$\begin{aligned} & \text{trace}(\mathbf{Q}\mathbf{L}\mathbf{Q}^T) \\ &= \text{trace}(\mathbf{Q}^T \mathbf{Q}\mathbf{L}) \\ &= \begin{pmatrix} \mathbf{Q}_Y^T \mathbf{Q}_Y & \mathbf{Q}_Y^T \mathbf{Q}_A \\ \mathbf{Q}_A^T \mathbf{Q}_Y & \mathbf{Q}_A^T \mathbf{Q}_A \end{pmatrix} \begin{pmatrix} \mathbf{I} & -\mathbf{X}^T \\ -\mathbf{X} & \text{diag}(\mathbf{X}\mathbf{1}) \end{pmatrix} \\ &= \text{trace}((\mathbf{Q}_Y^T \mathbf{Q}_Y)\mathbf{I} - \mathbf{Q}_Y^T \mathbf{Q}_A \mathbf{X} - \mathbf{Q}_A^T \mathbf{Q}_Y \mathbf{X}^T - \mathbf{Q}_A^T \mathbf{Q}_A \mathbf{G}) \\ &= \text{trace}(\mathbf{X}^T \mathbf{Q}_A^T \mathbf{Q}_A \mathbf{X} - 2\mathbf{X}^T \mathbf{Q}_A^T \mathbf{Q}_A \mathbf{X} - \mathbf{Q}_A^T \mathbf{Q}_A \mathbf{G}) \\ &= \text{trace}(\mathbf{Q}_A^T \mathbf{Q}_A (\mathbf{G} - \mathbf{X}^T \mathbf{X})) = \text{trace}(\mathbf{Q}_A \mathbf{L}_A \mathbf{Q}_A^T), \end{aligned}$$

where $\mathbf{G} = \text{diag}(\mathbf{X}\mathbf{1})$ and \mathbf{L}_A is known as the *Schur complement* of \mathbf{L} with respect to \mathbf{Y} .

It follows that the computation of the KDS spectral embedding only requires the calculation of the first k eigenvectors of the $m \times m$ matrix $\mathbf{X}\mathbf{X}^T$, which is very small since $m \ll n$, as well as a handful of $O(mn)$ -time multiplications by the matrix \mathbf{X} to compute the adjacency matrix $\mathbf{X}\mathbf{X}^T$ and recover $\mathbf{Q}_Y = \mathbf{Q}_A \mathbf{X}$. This observation will be later leveraged for efficient spectral clustering.

5 Dictionary learning algorithm

In the previous section, we have established identifiability of sparse codes using the weighted ℓ_1 regularization assuming a certain generative model of data. In practice, we only have access to a set of data points and need to estimate both the sparse representations and dictionary atoms. To this end, we study the following minimization problem.

$$\min_{\mathbf{A} \in \mathcal{R}^{d \times m}, \mathbf{X} \in S} \sum_{i=1}^n \left[\frac{1}{2} \|\mathbf{y}_i - \mathbf{A}\mathbf{x}_i\|^2 + \lambda \sum_{j=1}^m x_{ij} \|\mathbf{y}_i - \mathbf{a}_j\|^2 \right], \quad (6)$$

where $\mathbf{X} = [\mathbf{x}_1, \mathbf{x}_2, \dots, \mathbf{x}_n]$ with each $\mathbf{x}_i \in \Delta^m$. The balance between the reconstruction loss and the locality regularization is controlled by the parameter λ which in turn determines the sparsity of \mathbf{X} . A standard way to solve the above minimization program is alternating minimization which alternates between sparse approximation and dictionary update step [4]. We discuss the two steps below. The KDS algorithm is summarized in in Algorithm 1.

5.1 Sparse coding

Given a fixed dictionary \mathbf{A} , the sub-problem over the sparse coefficients is a weighted ℓ_1 minimization problem for which efficient methods exist [55]. We discuss two methods to solve this problem. The first method is the accelerated projected gradient descent algorithm [10] and the second method is the Frank-Wolfe algorithm [23]. Since the minimization problem for \mathbf{X} decouples into optimizing the sparse representation of each data point, we consider the problem of finding the optimal coefficient given the dictionary \mathbf{A} and a data point \mathbf{y}

$$\mathbf{x}^*(\mathbf{A}, \mathbf{y}) = \underset{\mathbf{x} \in \Delta^m}{\text{argmin}} \frac{1}{2} \|\mathbf{y} - \mathbf{A}\mathbf{x}\|^2 + \lambda \sum_{j=1}^m x_j \|\mathbf{y} - \mathbf{a}_j\|^2, \quad (7)$$

Let $\mathcal{L}(\mathbf{A}, \mathbf{y}, \mathbf{x}, \lambda)$ denote the objective in the above program.

The accelerated projected gradient descent: This method starts with the initialization $\mathbf{x}^0 = \tilde{\mathbf{x}}^{(0)} = \mathbf{0}$ and considers the following updates

$$\begin{aligned} \mathbf{x}^{(t+1)} &= \mathcal{P}_S \left(\tilde{\mathbf{x}}^{(t)} - \alpha \nabla_{\mathbf{x}} \mathcal{L}(\mathbf{A}, \mathbf{y}, \tilde{\mathbf{x}}^{(t)}) \right) \\ \tilde{\mathbf{x}}^{(t+1)} &= \mathbf{x}^{(t+1)} + \gamma^{(t)} (\mathbf{x}^{(t+1)} - \mathbf{x}^{(t)}), \end{aligned}$$

for $0 \leq t \leq T$. The operator \mathcal{P}_S projects onto S , the probability simplex and has a closed form that can be readily computed [70, 16]. The parameter α is a step size, and the constants $\gamma^{(t)}$ are given by the recurrence

$$\eta^{(0)} = 0, \eta^{(t+1)} = \frac{1 + \sqrt{1 + 4\eta^{(t)}}}{2}, \gamma^{(t)} = \frac{\eta^{(t)} - 1}{\eta^{(t+1)}}.$$

We note below the gradient of \mathcal{L} with respect to \mathbf{x}_i

$$\nabla_{\mathbf{x}_i} \mathcal{L}(\mathbf{A}, \mathbf{y}_i, \mathbf{x}_i, \lambda) = \mathbf{A}^\top (\mathbf{A} \mathbf{x}_i - \mathbf{y}_i) + \lambda \sum_{j=1}^m \|\mathbf{y}_i - \mathbf{a}_j\|^2 \mathbf{e}_j.$$

Frank-Wolfe: Frank-Wolfe is a projection-free first order optimization algorithm for optimizing a convex program over a compact convex set. In our setting, the objective in (7) is convex and S is a compact convex set. Given an initialization $\mathbf{x}^0 \in S$, the basic Frank-Wolfe algorithm considers the following iterates for $t \geq 0$ [32]

$$\begin{aligned} \mathbf{s} &= \arg \min_{\mathbf{s} \in S} \langle \mathbf{s}, \nabla_{\mathbf{x}} \mathcal{L}(\mathbf{x}^{(t)}) \rangle, \\ \mathbf{x}^{(t+1)} &= (1 - \gamma^{(t)}) \mathbf{x}^{(t)} + \gamma \mathbf{s}, \quad \text{for } \gamma^{(t)} = \frac{2}{t+2} \end{aligned}$$

The first optimization over the probability simplex S is a direction finding sub-problem. The optimal solution is $\mathbf{s} = \mathbf{e}_j$ where $j = \arg \min_{1 \leq i \leq m} (\nabla_{\mathbf{x}} \mathcal{L}(\mathbf{x}^{(t)})_i)$. Compared to the projection based approach which costs $O(m \log(m))$, the direction finding sub-problem is only $O(m)$. In addition, an appeal of the Frank-Wolfe is that the iterates are sparse as the directions are extreme points of S [32]. However, a drawback is the slow convergence rate of $O(1/t)$.

5.2 Dictionary learning

After carrying the sparse coding step for T iterations, we have optimized sparse coefficients $\{\mathbf{x}_i^{(T)}\}_{i=1}^n$ corresponding to the data points $\{\mathbf{y}_i\}_{i=1}^n$. The next part of the algorithm is to optimize for the dictionary which can be estimated by solving the following optimization problem

$$\min_{\mathbf{A} \in \mathcal{R}^{d \times m}} \sum_{i=1}^n \left[\frac{1}{2} \|\mathbf{y}_i - \mathbf{A} \mathbf{x}_i^{(T)}\|^2 + \lambda \sum_{j=1}^m x_{ij}^{(T)} \|\mathbf{y}_i - \mathbf{a}_j\|^2 \right], \quad (8)$$

The gradient of the summand of the loss function in (8) with respect to \mathbf{A} is given by $\nabla_{\mathbf{A}} \mathcal{L}(\mathbf{A}, \mathbf{y}_i, \mathbf{x}_i) = (\mathbf{A} \mathbf{x}_i - \mathbf{y}_i) \mathbf{x}_i^\top + 2\lambda \sum_{j=1}^m (\mathbf{x}_i^{(T)})_j (\mathbf{a}_j - \mathbf{y}_i)$. We note that the dictionary learning sub-problem is solved using a single step of gradient descent.

Complexity: For a fixed data point, the gradient update to estimate the coefficient is $O(md)$ and the projection onto the simplex is $O(m \log(m))$ [70]. Therefore, the per-iteration cost of sparse coding is $O(nm \max(\log(m), d))$. The complexity of the dictionary learning step is $O(nmd)$ which is the cost of the gradient update. An advantage of the proposed algorithm is that the sparse coding step is suited to GPU parallelizations across the data points.

Algorithm 1 KDS algorithm to solve (6)

- 1: **Input:** Data points $\mathbf{Y} = [\mathbf{y}_1, \dots, \mathbf{y}_n] \in \mathcal{R}^{d \times n}$, maxiterations.
 - 2: **Initialization:** $\mathbf{x}_i^0 = \mathbf{0}$ for $1 \leq i \leq n$. Set $\mathbf{A}^{(0)}$ to be random subset of data.
 - 3: **for** $k = 1$:maxiterations **do**
 - 4: Set step size: $\alpha = \frac{1}{(\sigma_{\max}(\mathbf{A}^{(k-1)}))^2}$.
 - 5: **Sparse coding via Encoder:** Given $\mathbf{A}^{(k-1)}$, use accelerated project gradient descent to obtain $\{\mathbf{x}_1^{(k)}, \mathbf{x}_2^{(k)}, \dots, \mathbf{x}_n^{(k)}\}$.
 - 6: **Decoder:** Reconstruct approximate data $\{\mathbf{A}^{(k-1)} \mathbf{x}_1^{(k)}, \dots, \mathbf{A}^{(k-1)} \mathbf{x}_n^{(k)}\}$.
 - 7: **Dictionary learning:** Backpropagation to obtain $\mathbf{A}^{(k)}$.
-

5.3 Algorithm unrolling

In order to solve (6) efficiently and to design an interpretable network, we consider an alternate strategy via a technique known as algorithm unrolling. This is the process of designing highly-structured recurrent neural network to efficiently solve problems [48]. Although our application of the technique for manifold learning is new, there exists a rich literature on the subject in the context of sparse dictionary learning [12, 27, 53, 63, 64, 65, 62]. In order to solve the relaxed optimization problem in (8), we introduce an autoencoder architecture that implicitly solves the problem when trained by backpropagation. Given a dictionary \mathbf{A} , our encoder maps a data point \mathbf{y} , or a batch of such points, to the sparse code \mathbf{x} minimizing $\mathcal{L}(\mathbf{A}, \mathbf{y}, \mathbf{x})$. This is done by unfolding T iterations of projected gradient descent on \mathcal{L} into a deep recurrent neural network. Our linear decoder reconstructs the input as $\hat{\mathbf{y}} = \mathbf{A} \mathbf{x}$. The network weights correspond to the dictionary \mathbf{A} , which is initialized to a random subset of the data \mathbf{Y} and then trained to minimize (6) by backpropagation through the entire autoencoder. If we view the forward pass through our encoder as an analogue of the sparse recovery step used in traditional alternating-minimization schemes, then this backward pass corresponds to an enhanced version of the so-called ‘‘dictionary update’’ step. We note that the projection onto the probability simplex can be written as $\mathcal{P}_S(\mathbf{x}) = \text{ReLU}(\mathbf{x} + b(\mathbf{x}) \cdot \mathbf{1})$ for an efficiently computable, piecewise-linear bias function $b: \mathcal{R}^m \rightarrow \mathcal{R}$ and thus serves as a non-linear activation function in the encoder.

6 Application of KDS to clustering

Let $\mathbf{Y} = [\mathbf{y}_1, \dots, \mathbf{y}_n] \in \mathcal{R}^{d \times n}$ be a collection of n data points in \mathcal{R}^d . To cluster the data, we utilize the algorithm discussed in Section 5 and obtain sparse representation coefficients \mathbf{X} and a set of m atoms $\mathbf{a}_1, \dots, \mathbf{a}_m$. Using the coefficients \mathbf{X} , we can construct a similarity graph on the $n + m$ data points and atoms $\mathbf{y}_1, \dots, \mathbf{y}_n, \mathbf{a}_1, \dots, \mathbf{a}_m \in \mathcal{R}^d$ by including an edge of weight x_{ij} between each data point \mathbf{y}_i and each atom \mathbf{a}_j . Given the similarity graph, to cluster the data, we apply spectral clustering, which first embeds the data using the first eigenvectors of a normalized graph Laplacian and runs k -means on the embeddings to obtain the cluster labels [50]. In the following subsection, we provide theoretical guarantees of the proposed framework for the clustering task under some assumptions on the data model.

6.1 Generative model

We consider m landmark points $\mathbf{a}_1, \mathbf{a}_2, \dots, \mathbf{a}_m$ with a unique Delaunay triangulation. In this setting, each point in the set $\{\mathbf{y}_i\}_{i=1}^n \in \mathcal{R}^d$ is generated from a convex combination of at most $d + 1$ atoms. For simplicity of presentation, we assume there are two clusters. The notion of connectedness is important to analysis of clustering guarantees and we state the following definition in the context of the Delaunay triangulation.

Definition 4. Given a set of n points $\{\mathbf{q}_j\}_{j=1}^n$, we define a graph using an adjacency matrix as follows: $A_{i,j} = 1$ if \mathbf{q}_i and \mathbf{q}_j lie in the same or adjacent Delaunay triangles and $A_{i,j} = 0$ otherwise. We call the set of points Delaunay-connected if the induced graph is path connected.

Figure 3 shows an example with $d = 2$ i.e. data points in \mathcal{R}^2 which belong to two clusters and the set of points with each cluster are Delaunay-connected.

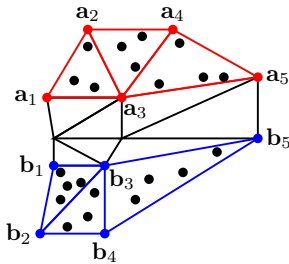


Figure 3: The red dots and blue dots indicate the atoms which define the first and second clusters respectively. Each black dot, denoting a data point, is a convex combination of three atoms which are vertices of the triangle the point belongs to. In this case, we see that each cluster is Delaunay-connected and there is no path between two points in different clusters.

Given the m landmark atoms, each data point in a triangle can be exactly expressed as a linear combination of the vertices of the triangle. We call the clustering exact if spectral clustering run on the similarity graph of these coefficients identifies the underlying clusters. A simple criterion to ensure that the clustering is exact is that the induced graphs of the two clusters are not Delaunay-connected i.e. there is no path between two points in different clusters.

Theorem 4. Consider a set of n points $\{\mathbf{y}_i\}_{i=1}^n$ generated from a convex combination of at most $(d + 1)$ -sparse atoms corresponding to the vertices of a Delaunay triangulation. Assume that there is an underlying clustering of the points into C_1, C_2 . Define the minimum separation distance between the clusters as $\Delta = \min_{i \in C_1, j \in C_2} \|\mathbf{y}_i - \mathbf{y}_j\|$. Let R be the maximum diameter of a triangle with the maximum taken among triangles that contain at least one point. If each cluster is Delaunay-connected and $\Delta > 2R$, spectral clustering identifies the two clusters exactly.

Proof of Theorem 1. $\Delta > 2R$ ensures that no triangle contains two points from different clusters. Using this and the fact that each of the clusters are Delaunay-connected, we conclude that spectral clustering identifies the clusters exactly. \square

We now consider a general model where the points are not necessarily exactly generated from the landmark points. Suppose each point in the first cluster is noisily generated using the dictionary $\mathbf{A} = [\mathbf{a}_1, \dots, \mathbf{a}_m]$ and each point in the second cluster is noisily generated using the dictionary $\mathbf{B} = [\mathbf{b}_1, \dots, \mathbf{b}_p]$. Let $\mathbf{D} = [\mathbf{A} \ \mathbf{B}]$. The points $[\mathbf{a}_1, \dots, \mathbf{a}_m]$ and $[\mathbf{b}_1, \dots, \mathbf{b}_p]$ are assumed to have a unique Delaunay triangulation. Consider a data point $\mathbf{y} = \sum_j x_j \mathbf{a}_j + \eta$ where η is additive noise. Assume ε -closeness of the data point \mathbf{y} in the dictionary \mathbf{A} i.e. there exist a representation coefficient \mathbf{x} such that $\|\mathbf{y} - \sum_j x_j \mathbf{a}_j\| \leq \varepsilon$. Further, assume also ε -closeness of the data point \mathbf{y} in the dictionary \mathbf{A}' where \mathbf{A}' consists of atoms from the dictionaries \mathbf{A} and \mathbf{B} . Of interest is the sense in which ε -closeness of the data point \mathbf{y} in the dictionary \mathbf{A} is optimal. To this end, we study the following optimization program

$$\begin{aligned} \min_{\mathbf{x} \in \mathcal{R}^{m+p}} \sum_j x_j \|\mathbf{y} - \mathbf{d}_j\|^2 \\ \text{s.t. } \|\mathbf{y} - \sum_j x_j \mathbf{d}_j\| \leq \varepsilon, \mathbf{x} \geq \mathbf{0} \text{ and } \mathbf{x}\mathbf{1} = \mathbf{1}, \end{aligned} \quad (9)$$

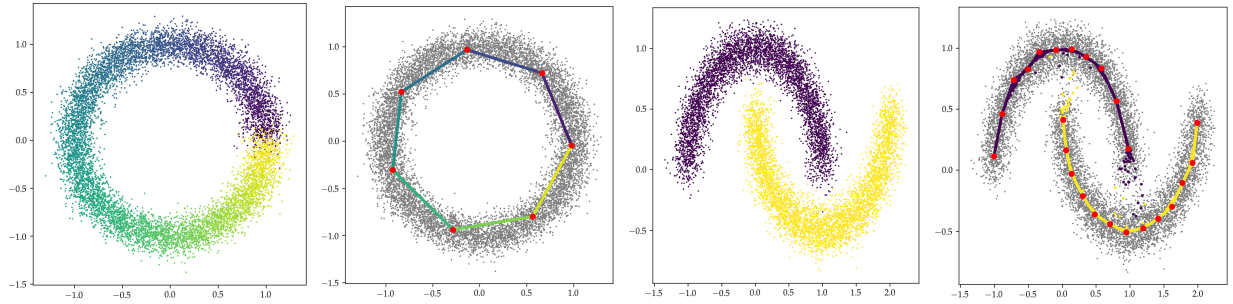


Figure 4: Circle and two moons. Autoencoder input (first and third) and output (second and fourth), with learned atoms marked in red.

where \mathbf{d}_j denotes the j -th column of the dictionary \mathbf{D} . We now define the following two quantities central to the main result to be stated below

$$\Delta_1 = \max_j \|\mathbf{y} - \mathbf{a}_j\|^2, \quad \Delta_2 = \min_j \|\mathbf{y} - \mathbf{a}'_j\|^2.$$

Theorem 5. *If $\Delta_2 > \Delta_1$, the optimal solution \mathbf{x}^* to the optimization program in (9) is such that it is nonzero only on indices corresponding to \mathbf{A} .*

Proof of Theorem 2. Assume an ε -close reconstruction of a point \mathbf{y} using the dictionary \mathbf{A}' . We consider the objective in (9)

$$\sum_j x_j \|\mathbf{y} - \mathbf{a}'_j\|^2 \geq \min_j \|\mathbf{y} - \mathbf{a}'_j\|^2 \sum_j x_j = \Delta_2 \cdot 1 = \Delta_2.$$

We now consider ε -close reconstruction of a point \mathbf{y} using the dictionary \mathbf{A} . We upper bound the objective in (9)

$$\sum_j x_j \|\mathbf{y} - \mathbf{a}_j\|^2 \leq \max_j \|\mathbf{y} - \mathbf{a}_j\|^2 \sum_j x_j \leq \Delta_1 \cdot 1 = \Delta_1.$$

Since $\Delta_2 > \Delta_1$, $\sum_j x_j \|\mathbf{y} - \mathbf{a}_j\|^2 < \sum_j x_j \|\mathbf{y} - \mathbf{a}'_j\|^2$. Therefore, the optimal solution to the optimization program in (9) is such that \mathbf{y} is ε -close in the dictionary \mathbf{A} . \square

Remark: The condition that $\Delta_2 > \Delta_1$ limits the type of cluster geometries that can be considered in the model. In the case that each cluster is densely sampled, the noise is small and the clusters are not wide relative to their separation, we expect $\Delta_2 > \Delta_1$ to hold. There are two possible avenues to improve the current analysis. First, the terms Δ_1 and Δ_2 do not interact with the noise. An ongoing analysis considers this and enforces that these terms depend on the bound on the noise. Second, our analysis hinges on ensuring that a data point does express itself using dictionary atoms that define the cluster it belongs too. This is not strictly necessary for the spectral clustering guarantee and we are currently studying the setup where a point could represent itself using atoms from a non-local dictionary.

Under the assumptions of Theorem 5, there is no path between points in the different clusters. Using the same arguments as in Theorem 4, if each cluster is Delaunay-connected, we can conclude that spectral clustering exactly identifies the clusters. The above analysis puts stringent conditions on the data points to obtain clustering performance guarantees. A future work is to consider a manifold clustering analysis such as in [7] to obtain non-uniform estimates that depend on local reconstruction (characterized by approximation of the manifold) and noise.

7 Experiments

In this section, we demonstrate the ability of KDS, implemented in PyTorch [51], to efficiently and accurately recover the underlying clusters of both synthetic and real-world data sets. Details about preprocessing of data and parameter selection for KDS as well as baseline algorithms can be found in the Appendix. All clustering experiments are evaluated with respect to a given ground truth clustering using the unsupervised clustering accuracy (ACC), which is invariant under a permutation of the cluster labels. Accuracy is defined the percentage of correct matches with respect to the ground truth labels of the data.

7.1 Synthetic Data

Learned Dictionary Atoms: For our first experiment, we qualitatively demonstrate the dictionary atoms learned by our autoencoder when the data is sampled from one-dimensional manifolds in \mathcal{R}^2 . Figure 4 shows two such data sets.

The first is the unit circle in \mathcal{R}^2 . The second is the classic two moon data set [50], which consists of two disjoint semicircular arcs in \mathcal{R}^2 . For each of these two data sets, we trained the autoencoder on data sampled uniformly from the underlying manifold(s). We added small Gaussian white noise to each data point to make the representation learning problem more challenging. Figure 4 shows the result of training the autoencoder on these data sets. We see that in each case, the atoms learned by the model are meaningful. Moreover, in each case, we accurately reconstruct each data point as sparse convex combinations of these atoms, up to the additive white noise. As a final remark, drawing a sample of 5000 data points from the noisy two moons distribution, computing their sparse coefficients, and performing spectral clustering with

$k = 2$ on the associated bipartite similarity graph results in a clustering accuracy of 100%. We note that KDS outperforms baseline algorithms (see Table 2).

Clustering with Narrow Separation: Our next experiment assesses the clustering capabilities of our algorithm in a toy setting. We studied a simple family of data distributions consisting of two underlying clusters in \mathcal{R}^2 . These clusters took the shape of two concentric circles of radii $r_{\text{outer}} = 1$ and $r_{\text{inner}} = 1 - \delta$, where $\delta \in [0, 1]$ is a separation parameter. For multiple values of δ , we trained our structured autoencoder with m atoms on an infinite stream of data sampled uniformly from these two manifolds, each with half the probability mass. For this experiment, we did not add any Gaussian noise to this data.

Figure 5 shows the results across a range of m and δ . Figure 6 shows the accuracy achieved by performing spectral clustering on the corresponding similarity graphs. Based on these results, it appears that our clustering algorithm is capable of distinguishing between clusters of arbitrarily small separation δ , provided that the number of atoms is sufficiently large; developing rigorous understanding of the dependence of m on δ is a topic of ongoing research.

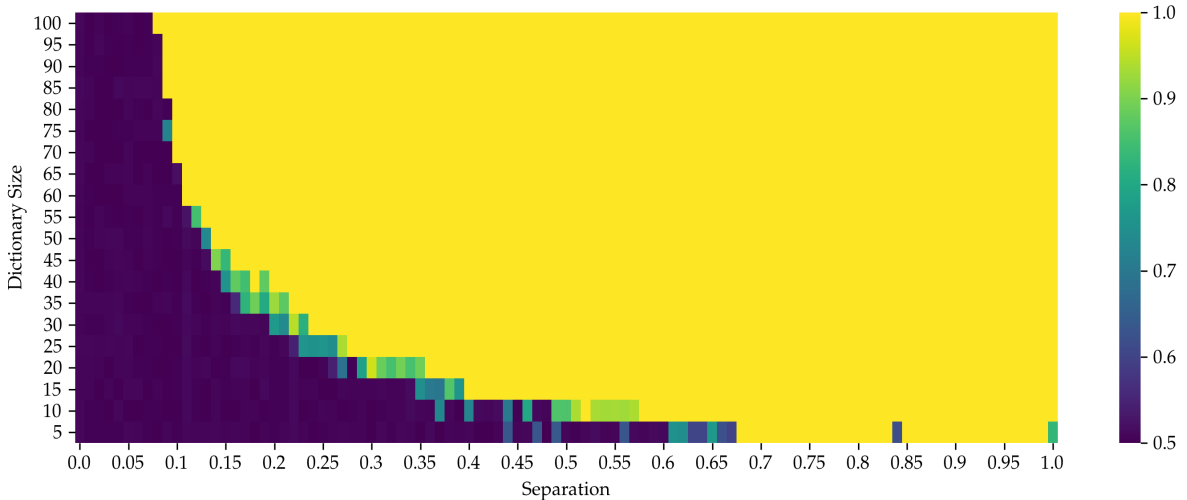


Figure 5: Clustering accuracy for concentric circles across δ, m .

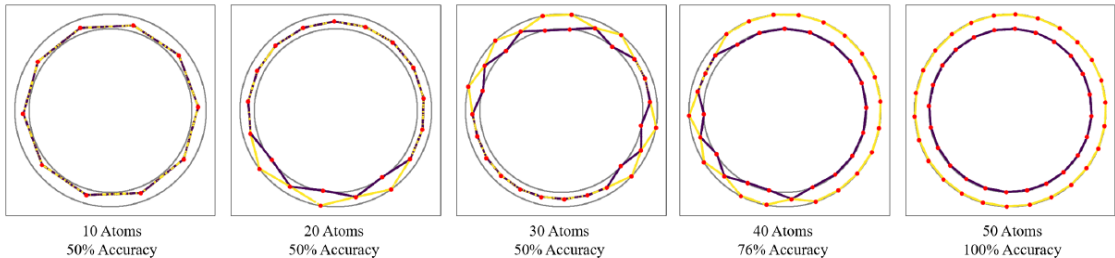


Figure 6: (a) Autoencoder output and learned atoms for concentric circles, separation $\delta = 0.15$.

7.2 Real-World Data

In this section, we empirically evaluate our algorithm on synthetic and three publicly available real-world data sets. We compared our method against two baseline clustering algorithms that may be interpreted as dictionary learning: (i) k -means (KM) [42], which learns a single dictionary atom for each cluster; (ii) SMCE, which solves a sparse optimization problem over a global dictionary consisting of all data points, then runs spectral clustering on a similarity graph derived from the solution [21]; (iii) LLE [68] which is a landmark method that uses uniform sampling (LLE-U) or k -means clustering (LLE-K) and (iv) LSC [75] is a landmark method that uses farthest first search. A summary of results can be found in Table 2. For LLE, clustering is based on an affinity matrix built from the weights. The reported accuracies are the best results after optimizing for different factors (# of neighbors, exemplar scheme, optimal clustering). Table 4 summarizes the number of exemplars used by KDS, LLE and LSC. We note that the linear system utilized in LLE is ill conditioned, due to few sample points to characterize the manifold, for the Yale B dataset and obtains poor results. We denote this result by NA. Similarly, clustering on MNIST is ill conditioned with 500 points and we instead set $m = 1000$.

Table 2: Clustering ACC for various data sets.

Method	Moons	MNIST-5	Yale B	SalinasA
KM	0.75	0.91	0.51	0.80
SMCE	0.88	0.94	1.0	0.85
KDS	1.0	0.99	1.0	0.88
LLE-U	0.907	0.97	NA	0.292
LLE-K	0.910	0.96	NA	0.285
LSC	0.87	0.51	0.91	0.28

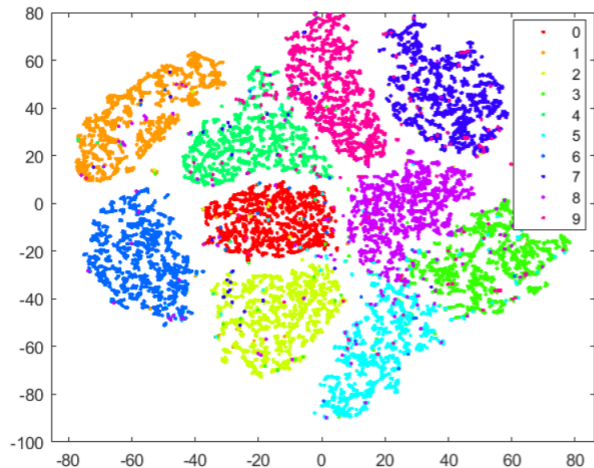


Figure 7: (t-SNE) plot of the KDS coefficients of the MNIST digits.

MNIST Handwritten Digit Database: The MNIST Handwritten Digit Database [34] consists of 28×28 grayscale images of 10 different digits. We ran our clustering on a subset of the data comprised of the $k = 5$ digits 0, 3, 4, 6, 7, following the example of [21]. Figure 1 shows a subset of the randomly initialized atoms for MNIST before training (black and white) and after training and clustering (color). Our results outperforms SMCE on this dataset.

MNIST-10: We run KDS on all digits of MNIST and obtain 86% accuracy. This is comparable to deep autoencoder-clustering methods [73, 71]. Compared to these baselines, we note that KDS is a structured framework and is more scalable and interpretable. In addition, we note that KDS is run on bare MNIST data with no feature extraction. A t-Distributed Stochastic Neighbor Embedding (t-SNE) [66] plot of the coefficients is shown in Figure 7. We can see that the digits are clustered based on their types.

Salinas-A Hyperspectral Image: The Salinas-A data set is a single aerial-view hyperspectral image of the Salinas valley in California with 224 bands and 6 regions corresponding to different crops [44]. We ran our algorithm on the entire 86×83 pixel image with $k = 6$ segments. We see an improvement in accuracy compared to SMCE.



Figure 8: SalinasA Scene. From left to right: image data (mean across spectral bands), ground truth clusters, predicted clusters.

Discussion: KDS exhibits excellent performance in accuracy while remaining scalable for large datasets. For the MNIST dataset (0,3,4,6,7) with 35037 digits, the total cost of KDS is only a few minutes. For SMCE, even with a small number of dictionary atoms, the computational cost is on the order of hours. Indeed, running SMCE on the MNIST dataset with a large number of nearest neighbors for each data point is infeasible on a standard laptop.

8 Conclusion

In this paper, we proposed a structured dictionary learning algorithm K-Deep Simplex (KDS) that combines nonlinear dimensionality reduction and sparse coding. Given a set of data points as an input, KDS learns a dictionary along with sparse coefficients supported on the probability simplex. Assuming that data points are generated from a convex combination of atoms, represented as vertices of a unique Delaunay triangulation, we prove that the proposed regularization recovers the underlying sparse solution. The optimization problem is recast and solved via a structured deep autoencoder. We then discuss how KDS can be applied for the clustering problem by constructing a similarity graph based on the obtained representation coefficients. Under a certain generative model, we provide performance guarantees for clustering. Our experiments show that KDS learns meaningful representation and obtains competitive results while offering dramatic savings in running time. In contrast to methods that set the dictionary to be the set of all data points, KDS is quasilinear with the number of dictionary atoms and offers a scalable framework. Future work will further explore the out-of-sample extension property of KDS and generative capabilities of the model.

Details of Numerical Experiments

In this section, we discuss how data are preprocessed and give algorithmic details about SMCE and KDS.

.1 Preprocessing of Data

We have preprocessed the input data in three different ways. The first is to simply scale the data to be in the range $[0, 1]$. The second is to standardize the data such it has mean 0 and standard deviation 1. The third way is to enforce that each data point has a unit norm. In reporting results for all methods, we have used these three preprocessings and reported the best result.

.2 SMCE Parameter Selection

The SMCE algorithm depends on a regularization parameter λ that controls the sparsity of the representation coefficients. For all of our numerical experiments, we considered $\lambda \in [1, 10, 100, 200]$ and report the best results. For both KDS and SMCE, the clustering accuracy is the best result among replicates of K-means run on the spectral embeddings.

.3 KDS Training and Parameter Selection

For each dataset (Moons, MNIST-5, YaleB, SalinasA), we trained KDS by backpropagation using the Adam optimizer for a fixed number of epochs. For all experiments, hyperparameters for KDS were chosen using an informal search of the parameter space with the goal of roughly balancing the two terms in the weighted ℓ_1 -regularized loss function. For the noisy two moons dataset, we unfolded our network for $T = 15$ layers, set $\lambda = 5.0$, set the Adam learning rate to 10^{-3} , and trained KDS for 10^3 epochs in batches of size 10^4 . For the MNIST-5 dataset, we unfolded our encoder for $T = 100$ layers, set $\lambda = 0.5$, set the learning rate to 10^{-3} , and trained KDS for 30 epochs in batches of size 1024. For the YaleB dataset, we unfolded our encoder for $T = 50$ layers, set $\lambda = 0.1$, set the learning rate to 10^{-4} , and trained KDS for 15 epochs in batches of size 1. Finally, for the SalinasA dataset, we unfolded our encoder for $T = 100$ layers, set $\lambda = 2.0$, set the learning rate to 10^{-4} , and trained KDS for 30 epochs in batches of size 128.

.4 Discussion of Clustering Experiments

To compare SMCE and KDS on the different datasets, we fix the number of dictionary atoms m . In the SMCE framework, this does imply that the optimization problem for each data point is based on a dictionary defined via the m neighbouring points. Table 3 lists the total number of data points and the number of atoms m used in our experiments. One could surmise that the SMCE results can be improved by increasing m or using a dictionary of all data points. In fact, our extensive numerical experiments indicate that the performance of SMCE or KDS depends on the intrinsic geometry which in turn is reflected by a judicious choice of m . For instance, if one uses 500 atoms for the Moons dataset for SMCE, the best obtained accuracy is 78.96% which is lower than an accuracy of 88% with 24 atoms. One remedy to this problem is to use a larger dictionary for SMCE but capture intrinsic geometry by tuning the proximity regularization parameter. A drawback of this is that SMCE is computationally expensive in this regime and the proposed procedure does not consistently yield improved results. We note that, while SMCE with a fixed m resembles KDS, there is a notable difference. In SMCE, each optimization problem uses local dictionaries while KDS employs a fixed learned global dictionary. In addition, in the regime m is small, one does no longer capture the global features learned from SMCE and the method is akin to nearest neighbour methods.

	Moons	MNIST-5	YaleB	SalinasA
n	5000	5000	128	7138
m	24	500	64	600

Table 3: The number of data points and number of atoms for different datasets used in our numerical experiments.

# of atoms	Moons	MNIST-5	Yale B	SalinasA
KDS	24	500	64	600
LLLE	24	1000	NA	600
LSC	24	500	64	600

Table 4: Number of landmark atoms.

.5 Choosing m

The number of dictionary atoms m is a central parameter of KDS. Because the dictionary is global, rather than local, it does not scale with the dimension of the data only. Indeed, m must be large enough to ensure that *any* observed data point is well-approximated by a sparse combination of the atoms. However, under the model that the data are sampled from a mixture of K probability measures supported on d -dimensional manifolds, m simply needs to be chosen large enough to provide an ε covering of the data. This can be done [28] taking $m = C\varepsilon^{-\frac{1}{d}} \log(\varepsilon^{-\frac{1}{d}})$, where C is a constant depending on the geometric properties of the underlying manifolds (e.g. their curvatures). Importantly, m can be taken independently from n and is “cursed” only by the intrinsic dimensionality of the data. This is most interesting in the case when n is

large. Indeed, if n is small, then $m = n$ is computationally tractable and taking a dictionary consisting of all observed data points will be optimal; this essentially reduces to the SMCE formulation.

Together, this suggests $m \ll n$ is possible for KDS while still achieving excellent performance, particularly when n is large. Our experimental results bear this out, especially for datasets with known low-dimensional structure. In the two moons data, for example, we take $m = 24$ even when $n = 5000$. This is possible because the intrinsic dimensionality of each moon is 1 in the noiseless case and approximately 1 in the presence of low-variance Gaussian noise.

References

- [1] Maryam Abdolali and Nicolas Gillis. Beyond linear subspace clustering: A comparative study of non-linear manifold clustering algorithms. *Computer Science Review*, 42:100435, 2021.
- [2] Maryam Abdolali and Nicolas Gillis. Simplex-structured matrix factorization: Sparsity-based identifiability and provably correct algorithms. *SIAM Journal on Mathematics of Data Science*, 3(2):593–623, 2021.
- [3] Maryam Abdolali, Nicolas Gillis, and Mohammad Rahmati. Scalable and robust sparse subspace clustering using randomized clustering and multilayer graphs. *Signal Processing*, 163:166–180, 2019.
- [4] Alekh Agarwal, Animashree Anandkumar, Prateek Jain, and Praneeth Netrapalli. Learning sparsely used overcomplete dictionaries via alternating minimization. *SIAM Journal on Optimization*, 26(4):2775–2799, 2016.
- [5] Michal Aharon, Michael Elad, and Alfred Bruckstein. K-svd: An algorithm for designing overcomplete dictionaries for sparse representation. *IEEE Transactions on signal processing*, 54(11):4311–4322, 2006.
- [6] William K Allard, Guangliang Chen, and Mauro Maggioni. Multi-scale geometric methods for data sets ii: Geometric multi-resolution analysis. *Applied and computational harmonic analysis*, 32(3):435–462, 2012.
- [7] Ery Arias-Castro, Gilad Lerman, and Teng Zhang. Spectral clustering based on local pca. *The Journal of Machine Learning Research*, 18(1):253–309, 2017.
- [8] Mikhail Belkin and Partha Niyogi. Laplacian eigenmaps for dimensionality reduction and data representation. *Neural computation*, 15(6):1373–1396, 2003.
- [9] Alfred M Bruckstein, David L Donoho, and Michael Elad. From sparse solutions of systems of equations to sparse modeling of signals and images. *SIAM review*, 51(1):34–81, 2009.
- [10] Sébastien Bubeck. Convex optimization: Algorithms and complexity. *Foundations and Trends® in Machine Learning*, 8(3-4):231–357, 2015.
- [11] Deng Cai, Xiaofei He, Jiawei Han, and Thomas S Huang. Graph regularized nonnegative matrix factorization for data representation. *IEEE transactions on pattern analysis and machine intelligence*, 33(8):1548–1560, 2010.
- [12] Thomas Chang, Bahareh Tolooshams, and Demba Ba. Randnet: deep learning with compressed measurements of images. In *2019 IEEE 29th International Workshop on Machine Learning for Signal Processing (MLSP)*, pages 1–6. IEEE, 2019.
- [13] Adam S Charles, Bruno A Olshausen, and Christopher J Rozell. Learning sparse codes for hyperspectral imagery. *IEEE Journal of Selected Topics in Signal Processing*, 5(5):963–978, 2011.
- [14] William S Cleveland. Robust locally weighted regression and smoothing scatterplots. *Journal of the American statistical association*, 74(368):829–836, 1979.
- [15] Ronald R Coifman and Stéphane Lafon. Diffusion maps. *Applied and computational harmonic analysis*, 21(1):5–30, 2006.
- [16] Laurent Condat. Fast projection onto the simplex and the l1 ball. *Mathematical Programming*, 158(1):575–585, 2016.
- [17] Adele Cutler and Leo Breiman. Archetypal analysis. *Technometrics*, 36(4):338–347, 1994.
- [18] Vin De Silva and Joshua B Tenenbaum. Sparse multidimensional scaling using landmark points. Technical report, technical report, Stanford University, 2004.
- [19] Chris HQ Ding, Tao Li, and Michael I Jordan. Convex and semi-nonnegative matrix factorizations. *IEEE transactions on pattern analysis and machine intelligence*, 32(1):45–55, 2008.
- [20] Fadi Dornaika and Libo Weng. Sparse graphs with smoothness constraints: Application to dimensionality reduction and semi-supervised classification. *Pattern Recognition*, 95:285–295, 2019.
- [21] Ehsan Elhamifar and René Vidal. Sparse manifold clustering and embedding. *Advances in neural information processing systems*, 24:55–63, 2011.
- [22] Kjersti Engan, Sven Ole Aase, and John Håkon Husøy. Multi-frame compression: Theory and design. *Signal Processing*, 80(10):2121–2140, 2000.

- [23] Marguerite Frank and Philip Wolfe. An algorithm for quadratic programming. *Naval Research Logistics Quarterly*, 3(1-2):95–110, 1956.
- [24] Jerome H Friedman and Werner Stuetzle. Projection pursuit regression. *Journal of the American statistical Association*, 76(376):817–823, 1981.
- [25] N. Gillis. *Nonnegative Matrix Factorization*. Data Science. Society for Industrial and Applied Mathematics, 2020.
- [26] John B Greer. Sparse demixing of hyperspectral images. *IEEE Transactions on image processing*, 21(1):219–228, 2011.
- [27] Karol Gregor and Yann LeCun. Learning fast approximations of sparse coding. In *Proceedings of the 27th international conference on international conference on machine learning*, pages 399–406, 2010.
- [28] László Györfi, Michael Kohler, Adam Krzyzak, and Harro Walk. *A distribution-free theory of nonparametric regression*. Springer Science & Business Media, 2006.
- [29] David Hallac, Jure Leskovec, and Stephen Boyd. Network lasso: Clustering and optimization in large graphs. In *Proceedings of the 21th ACM SIGKDD international conference on knowledge discovery and data mining*, pages 387–396, 2015.
- [30] Han Hu, Zhouchen Lin, Jianjiang Feng, and Jie Zhou. Smooth representation clustering. In *Proceedings of the IEEE conference on computer vision and pattern recognition*, pages 3834–3841, 2014.
- [31] Jin Huang, Feiping Nie, and Heng Huang. A new simplex sparse learning model to measure data similarity for clustering. In *Twenty-fourth international joint conference on artificial intelligence*, 2015.
- [32] Martin Jaggi. Revisiting frank-wolfe: Projection-free sparse convex optimization. In *International Conference on Machine Learning*, pages 427–435. PMLR, 2013.
- [33] Kun Jiang, Zhaoli Liu, Zheng Liu, and Qindong Sun. Locality constrained analysis dictionary learning via k-svd algorithm. *arXiv preprint arXiv:2104.14130*, 2021.
- [34] Yann LeCun, Léon Bottou, Yoshua Bengio, and Patrick Haffner. Gradient-based learning applied to document recognition. *Proceedings of the IEEE*, 86(11):2278–2324, 1998.
- [35] Daniel D Lee and H Sebastian Seung. Learning the parts of objects by non-negative matrix factorization. *Nature*, 401(6755):788–791, 1999.
- [36] Der-Tsai Lee and Bruce J Schachter. Two algorithms for constructing a delaunay triangulation. *International Journal of Computer & Information Sciences*, 9(3):219–242, 1980.
- [37] John M Lee. Smooth manifolds. In *Introduction to Smooth Manifolds*, pages 1–31. Springer, 2013.
- [38] Bin Li, J Friedman, R Olshen, and C Stone. Classification and regression trees (cart). *Biometrics*, 40(3):358–361, 1984.
- [39] Wenjing Liao, Mauro Maggioni, and Stefano Vignola. Multiscale regression on unknown manifolds. *Mathematics in Engineering*, 4(4):1–25, 2022.
- [40] Chia-Hsiang Lin, Ruiyuan Wu, Wing-Kin Ma, Chong-Yung Chi, and Yue Wang. Maximum volume inscribed ellipsoid: A new simplex-structured matrix factorization framework via facet enumeration and convex optimization. *SIAM Journal on Imaging Sciences*, 11(2):1651–1679, 2018.
- [41] Wei Liu, Junfeng He, and Shih-Fu Chang. Large graph construction for scalable semi-supervised learning. In *Proceedings of the 27th International Conference on International Conference on Machine Learning*, page 679–686, Madison, WI, USA, 2010. Omnipress.
- [42] Stuart Lloyd. Least squares quantization in pcm. *IEEE transactions on information theory*, 28(2):129–137, 1982.
- [43] Clive Loader. *Local regression and likelihood*. Springer Science & Business Media, 2006.
- [44] B Ayerdi M Graña, MA Veganzons. Hyperspectral remote sensing scenes. http://www.ehu.es/ccwintco/index.php/Hyperspectral_Remote_Sensing_Scenes. Accessed: 2020-02-04.
- [45] Mauro Maggioni, Stanislav Minsker, and Nate Strawn. Multiscale dictionary learning: non-asymptotic bounds and robustness. *The Journal of Machine Learning Research*, 17(1):43–93, 2016.
- [46] Shin Matsushima and Maria Brbic. Selective sampling-based scalable sparse subspace clustering. *Advances in Neural Information Processing Systems*, 32, 2019.
- [47] Dermot H McLain. Drawing contours from arbitrary data points. *The Computer Journal*, 17(4):318–324, 1974.
- [48] Vishal Monga, Yuelong Li, and Yonina C. Eldar. Algorithm Unrolling: Interpretable, Efficient Deep Learning for Signal and Image Processing. *arXiv e-prints*, 2019.
- [49] Vishal Monga, Yuelong Li, and Yonina C Eldar. Algorithm unrolling: Interpretable, efficient deep learning for signal and image processing. *IEEE Signal Processing Magazine*, 38(2):18–44, 2021.

- [50] Andrew Ng, Michael Jordan, and Yair Weiss. On spectral clustering: Analysis and an algorithm. *Advances in neural information processing systems*, 14:849–856, 2001.
- [51] Adam Paszke, Sam Gross, Francisco Massa, Adam Lerer, James Bradbury, Gregory Chanan, Trevor Killeen, Zeming Lin, Natalia Gimelshein, Luca Antiga, et al. Pytorch: An imperative style, high-performance deep learning library. *Advances in Neural Information Processing Systems*, 32:8026–8037, 2019.
- [52] Mathis Petrovich and Makoto Yamada. Fast local linear regression with anchor regularization. *arXiv preprint arXiv:2003.05747*, 2020.
- [53] Jason Tyler Rolfe and Yann LeCun. Discriminative recurrent sparse auto-encoders: 1st international conference on learning representations, iclr 2013. In *1st International Conference on Learning Representations, ICLR 2013*, 2013.
- [54] Sam T Roweis and Lawrence K Saul. Nonlinear dimensionality reduction by locally linear embedding. *science*, 290(5500):2323–2326, 2000.
- [55] M. Salman Asif and Justin Romberg. Fast and Accurate Algorithms for Re-Weighted L1-Norm Minimization. *arXiv e-prints*, 2012.
- [56] Bernhard Schölkopf, Alexander Smola, and Klaus-Robert Müller. Kernel principal component analysis. In *International conference on artificial neural networks*, pages 583–588. Springer, 1997.
- [57] Vin Silva and Joshua Tenenbaum. Global versus local methods in nonlinear dimensionality reduction. *Advances in neural information processing systems*, 15:721–728, 2002.
- [58] Charles J Stone. Consistent nonparametric regression. *The annals of statistics*, pages 595–620, 1977.
- [59] Pranay Tankala, Abiy Tasissa, James M Murphy, and Demba Ba. K-deep simplex: Deep manifold learning via local dictionaries. *arXiv preprint arXiv:2012.02134*, 2020.
- [60] Abiy Tasissa, Pranay Tankala, and Demba Ba. Weighed l1 on the simplex: Compressive sensing meets locality. In *2021 IEEE Statistical Signal Processing Workshop (SSP)*, pages 476–480, 2021.
- [61] Joshua B Tenenbaum, Vin De Silva, and John C Langford. A global geometric framework for nonlinear dimensionality reduction. *science*, 290(5500):2319–2323, 2000.
- [62] Bahareh Tolooshams and Demba Ba. Stable and interpretable unrolled dictionary learning. *Transactions on Machine Learning Research*, 2022.
- [63] Bahareh Tolooshams, Sourav Dey, and Demba Ba. Scalable convolutional dictionary learning with constrained recurrent sparse auto-encoders. In *2018 IEEE 28th International Workshop on Machine Learning for Signal Processing (MLSP)*, pages 1–6. IEEE, 2018.
- [64] Bahareh Tolooshams, Sourav Dey, and Demba Ba. Deep residual autoencoders for expectation maximization-inspired dictionary learning. *IEEE Transactions on Neural Networks and Learning Systems*, 2020.
- [65] Bahareh Tolooshams, Andrew Song, Simona Temereanca, and Demba Ba. Convolutional dictionary learning based auto-encoders for natural exponential-family distributions. In *International Conference on Machine Learning*, pages 9493–9503. PMLR, 2020.
- [66] Laurens Van der Maaten and Geoffrey Hinton. Visualizing data using t-sne. *Journal of machine learning research*, 9(11), 2008.
- [67] David van Dijk, Daniel B Burkhardt, Matthew Amodio, Alexander Tong, Guy Wolf, and Smita Krishnaswamy. Finding archetypal spaces using neural networks. In *2019 IEEE International Conference on Big Data (Big Data)*, pages 2634–2643. IEEE, 2019.
- [68] Max Vladymyrov and Miguel Á Carreira-Perpinán. Locally linear landmarks for large-scale manifold learning. In *Joint European Conference on Machine Learning and Knowledge Discovery in Databases*, pages 256–271. Springer, 2013.
- [69] Jinjun Wang, Jianchao Yang, Kai Yu, Fengjun Lv, Thomas Huang, and Yihong Gong. Locality-constrained linear coding for image classification. In *2010 IEEE computer society conference on computer vision and pattern recognition*, pages 3360–3367. IEEE, 2010.
- [70] Weiran Wang and Miguel A Carreira-Perpinán. Projection onto the probability simplex: An efficient algorithm with a simple proof, and an application. *arXiv preprint arXiv:1309.1541*, 2013.
- [71] Junyuan Xie, Ross Girshick, and Ali Farhadi. Unsupervised deep embedding for clustering analysis. In *International conference on machine learning*, pages 478–487. PMLR, 2016.
- [72] Makoto Yamada, Takeuchi Koh, Tomoharu Iwata, John Shawe-Taylor, and Samuel Kaski. Localized lasso for high-dimensional regression. In *Artificial Intelligence and Statistics*, pages 325–333. PMLR, 2017.
- [73] Bo Yang, Xiao Fu, Nicholas D Sidiropoulos, and Mingyi Hong. Towards k-means-friendly spaces: Simultaneous deep learning and clustering. In *international conference on machine learning*, pages 3861–3870. PMLR, 2017.

- [74] He-Feng Yin, Xiao-Jun Wu, and Su-Gen Chen. Locality constraint dictionary learning with support vector for pattern classification. *IEEE Access*, 7:175071–175082, 2019.
- [75] Chong You, Chi Li, Daniel P Robinson, and René Vidal. A scalable exemplar-based subspace clustering algorithm for class-imbalanced data. In *European Conference on Computer Vision*, pages 68–85. Springer, 2018.
- [76] Kai Yu, Tong Zhang, and Yihong Gong. Nonlinear learning using local coordinate coding. *Advances in neural information processing systems*, 22, 2009.
- [77] Miao Zheng, Jiajun Bu, Chun Chen, Can Wang, Lijun Zhang, Guang Qiu, and Deng Cai. Graph regularized sparse coding for image representation. *IEEE transactions on image processing*, 20(5):1327–1336, 2010.
- [78] Guo Zhong and Chi-Man Pun. Subspace clustering by simultaneously feature selection and similarity learning. *Knowledge-Based Systems*, 193:105512, 2020.
- [79] Yin Zhou and Kenneth E. Barner. Locality constrained dictionary learning for nonlinear dimensionality reduction. *IEEE Signal Processing Letters*, 20(4):335–338, 2013.